

# Growth differentiation factor-15 regulates oxLDL-induced lipid homeostasis and autophagy in human macrophages

Kathrin Ackermann\*, Gabriel A. Bonaterra, Ralf Kinscherf<sup>1</sup>, Anja Schwarz<sup>1</sup>

Institute for Anatomy and Cell Biology, Department of Medical Cell Biology, Philipps-University of Marburg, 35032, Marburg, Germany

## HIGHLIGHTS

- GDF-15 enhances oxLDL-independent lipid-accumulation in human MΦ.
- GDF-15 silencing in human MΦ inhibits oxLDL-induced lipid-accumulation.
- Incubation of human MΦ with rGDF-15/oxLDL increases ATG5, ATG12/ATG5-complex and p62.
- GDF-15 silencing in human MΦ reduces ATG5, ATG12/ATG5-complex and p62.
- GDF-15/oxLDL impairs autophagy with consequences for lipid homeostasis in human MΦ.

## ARTICLE INFO

**Keywords:**  
Autophagy  
p62  
ATG5  
GDF-15  
oxLDL

## ABSTRACT

**Background and aims:** Growth differentiation factor-15 (GDF-15)/macrophage inhibitory cytokine-1 (MIC-1/GDF15) is associated with cardiovascular disease, inflammation and development of atherosclerosis and is highly expressed in macrophages (MΦ) of atherosclerotic lesions. Thus, we were interested in investigating the influence of GDF-15 in lipid homeostasis and autophagy in human MΦ during foam cell formation.

**Methods and results:** Oxidized-low density lipoprotein (50 μg/ml oxLDL), recombinant (r)GDF-15, transiently silenced GDF-15 (*siGDF-15 MΦ*), as well as with negative siRNA transfected (*nsiGDF-15 MΦ*) PMA-differentiated human *THP-1 MΦ*, were used to investigate the effects of GDF-15 on autophagic processes and lipid accumulation. Oil Red O staining revealed that rGDF-15 alone, but also in combination with oxLDL, significantly increased the lipid accumulation in *THP-1 MΦ*; a reverse effect was detected in *siGDF-15 MΦ*. Western-blot analyses and confocal laser scanning microscopy showed an increase of Atg5, Atg12/Atg5 protein complex and p62 protein in *THP-1 MΦ* co-incubated with rGDF-15 and oxLDL, as well as an increase of p62 accumulation compared to rGDF-15-treated MΦ. *Vice versa*, *siGDF-15 MΦ* showed a reduced p62 accumulation compared to *nsiGDF-15 MΦ*. The present study indicates that GDF-15, especially in combination with oxLDL, regulates the expression of autophagy-relevant proteins (p62, Atg5 and Atg12/Atg5 protein complex) and p62 accumulation in human MΦ.

**Conclusions:** GDF-15, in combination with oxLDL, impairs autophagic processes with consequences for lipid homeostasis in human MΦ, indicating its novel important pathophysiological role in atherosclerotic plaque development and progression.

## 1. Introduction

Atherosclerosis, a chronic inflammation of the arterial wall, is accompanied by accumulation of lipids, inflammatory cells and foam cell formation. Studies have shown that elevated circulating levels of GDF-15 reflect endothelial activation and vascular inflammation, pathways regulating the development and progression of atherosclerosis [1]. In

general, increased serum cholesterol levels, especially low-density lipoprotein (LDL) cholesterol in the form of oxidized low-density lipoproteins (oxLDL), as well as macrophages (MΦ), play a key role in atherosclerotic processes, because MΦ internalize oxLDL via scavenger receptors and develop as foam cells. In this context, the growth differentiation factor-15 (GDF-15) is a divergent and distant member of the TGF-β superfamily, identical to the MΦ-inhibitory cytokine-1 (MIC-

\* Corresponding author.

E-mail addresses: [kathrin.ackermann@staff.uni-marburg.de](mailto:kathrin.ackermann@staff.uni-marburg.de) (K. Ackermann), [anja.schwarz@staff.uni-marburg.de](mailto:anja.schwarz@staff.uni-marburg.de) (A. Schwarz).

<sup>1</sup> These authors contributed to this work as senior authors.

1) [2,3]. Wide ranges of cell types express GDF-15, which acts as a pleiotropic cytokine and is involved in the response of cells after oxidative stress and cellular injury. GDF-15 is widely distributed in adult tissues, expressed in epithelial cells and M $\Phi$  [4,5]. GDF-15 expression is upregulated in mononuclear cells and/or M $\Phi$  by a variety of stimuli, including interleukin (IL)-1 $\beta$ , IL-2, tumor necrosis factor alpha (TNF $\alpha$ ), phorbol myristate acetate (PMA), retinoic acid (RA), ceramide, oxLDL, hydrogen peroxide or M $\Phi$ -colony-stimulating factor (M-CSF). Thus, GDF-15 seems to be associated with M $\Phi$  activation [1,2,6,7]. Though, increased GDF-15 protein levels are also associated with disease states such as tissue hypoxia, inflammation, acute injury and oxidative stress [5]. Therefore, it is noteworthy to mention that recent and older studies have shown that healthy women with higher serum GDF-15 levels are at increased risk of cardiovascular events [8,9]. However, the role of GDF-15 during the atherosclerotic processes is controversially discussed. On the one hand, GDF-15 deficiency has been shown to inhibit atherosclerosis progression in *ApoE*<sup>-/-</sup> mice after 20 weeks of high-fat diet [10]. On the other hand, transgenic overexpression of GDF-15 has been demonstrated to play a protective role in advanced stages of atherosclerosis in the *ApoE*<sup>-/-</sup> mouse model (after 6 months of high-fat diet) by observing the limitation or repair of atherosclerotic lesions [11]. Moreover, *in vitro* analyses of oxLDL-treated human M $\Phi$  showed an increased GDF-15 expression in addition to foam cell formation and apoptosis [7]. Processes of M $\Phi$ -derived foam cell formation and cell fate are associated with autophagy [12], which in general is an evolutionarily conserved mechanism and is important for numerous physiological and pathological processes [13]. Of note, clinical studies have shown a co-localization of autophagy-related proteins with M $\Phi$  in atherosclerotic plaques [14,15]. Nevertheless, the role of autophagy in the development and progression of atherosclerosis seems to be complex. It is known that in advanced stages of atherosclerosis, autophagy is impaired [14]. In this context, animal experiments using mice with M $\Phi$ -specific deletion of the autophagy gene *Atg5* have recently shown that these mice developed plaques with increased apoptosis, as well as oxidative stress, and exhibited enhanced plaque necrosis [16].

Because the role of GDF-15 during the development of atherosclerosis is diversely discussed [10,11,17], a relation between GDF-15, apoptosis, as well as autophagy and atherosclerosis development/progression, may be suggested due to histomorphometrical data of atherosclerotic lesions [10]. We aimed to decipher the role of GDF-15 in the formation of foam cells with respect to autophagy in oxLDL-treated human M $\Phi$ .

## 2. Materials and methods

### 2.1. LDL-oxidation

Native (n)LDL (RayBiotech, GA, USA) oxidation was performed as previously described by Galle and Wanner [18] and Steinbrecher [19]. nLDL was suspended in endotoxin-free phosphate-buffered saline (PBS) without Ca<sup>2+</sup>, Mg<sup>2+</sup> (LONZA, Ratingen, Germany) to a final concentration of 1 mg protein/ml, and dialyzed using Slide-A-Lyzer Dialysis Cassettes 7K MWCO (Thermo Fisher Scientific Inc., Rockford, USA). OxLDL was obtained by oxidizing nLDL using CuSO<sub>4</sub> (50  $\mu$ M in PBS Ca<sup>2+</sup>, Mg<sup>2+</sup> free, 24 h, RT). Different methods verified the grade of oxidation: (1) trinitrobenzene sulfonic acid (TNBSA, Thermo Fisher Scientific Inc., Rockford, USA), which measures free amino groups [20], (2) relative electrophoretic mobility (REM) by agarose gel electrophoresis and visualization by staining with Coomassie Blue [21], and (3) spectrophotometric analysis (absorbance spectrum between 400 and 700 nm [18]). OxLDL was used by an increased REM of 17.5%  $\pm$  3.34% compared to nLDL, an increased percentage of blocked amino groups (40.4%  $\pm$  0.65% compared to LDL) and by the disappearance of the nLDL characteristic absorption peaks at 460 and 485 nm [18] (Supplemental Fig. 1).

### 2.2. Cell culture, transfection and gene silencing

The human leukemic monocyte cell line *THP-1* (Leibniz Institute DSMZ, Braunschweig, Germany) was used. Originally, the culture was derived from the blood of a one-year old boy with acute monocytic leukemia and is frequently used as a model of monocyte/M $\Phi$  cell lineage [22]. *THP-1* cells were cultured in RPMI-1640 medium (Capricorn Scientific GmbH, Ebsdorfergrund, Germany) supplemented with penicillin and streptomycin (Capricorn Scientific GmbH) and 10% fetal bovine serum (Capricorn Scientific GmbH). Cells were cultured at 37 °C in a 5% CO<sub>2</sub> environment, with a medium change every 2–3 days. All experiments were performed using cells at passage 9 and lower. RPMI 1640 medium supplemented with 100 nM phorbol 12-myristate 13-acetate [PMA, (Sigma-Aldrich Chemie GmbH Munich, Germany)] was used (72 h) in *THP-1* cells to induce monocyte differentiation into M $\Phi$ . Transfection of *THP-1* M $\Phi$  with 50 nM small interfering RNA (siRNA) for *GDF-15* (FlexiTube GeneSolution GS9518, QIAGEN GmbH, Hilden, Germany) and with negative siRNA (*nsiGDF-15*) (AllStars Negative Control, QIAGEN GmbH) was performed using HiPerfect Transfection Reagent (QIAGEN GmbH) following the manufacturer's instructions. As positive control, we used the AllStars Hs Cell Death Control siRNA (QIAGEN GmbH), a compound of highly potent siRNAs targeting ubiquitously expressed human genes that are essential for cell survival. Transfection efficiency was estimated by observing cells by light microscopy 48 h after transfection with the AllStars Hs Cell Death Control siRNA. After transfection, cells were treated with 50  $\mu$ g/ml oxLDL to induce foam cell formation or were left untreated (medium) for 4 h. Because of the biological activity of rGDF-15 ED50 = 1.0–3.0  $\mu$ g/ml (ProViro, Germany), PMA-differentiated *THP-1* M $\Phi$  were treated with 1.0–1.5  $\mu$ g/ml human rGDF-15 [rGDF-15 (ProViro AG, Berlin, Germany)] or co-incubated with oxLDL + rGDF-15 for 4 h.

### 2.3. GDF-15 ELISA

The intracellular level of human GDF-15 was quantified by the DuoSet<sup>®</sup> ELISA Development System (R&D Systems, Inc., Abingdon, UK). The Capture Antibody was coated to a 96-well MaxiSorp-ELISA Microplate (Nunc, San Diego, USA) and incubated overnight at room temperature. According to manufacturers' instructions, after the blocking step, the samples (2.5  $\mu$ g protein/well) or standards were added into the well. After the incubation with a detection antibody and streptavidin-HRP, we added the substrate solution (SigmaFast<sup>™</sup> OPD, Sigma-Aldrich Chemie GmbH) to each well and incubated for 30 min in the dark. The reaction was stopped with 50  $\mu$ l 3 M HCl. The GDF-15 protein level (pg/ml) was measured with an ELISA reader (Tecan Deutschland GmbH, Crailsheim, Germany) at OD<sub>490/655 nm</sub>.

### 2.4. SDS-PAGE and Western blot

After the treatments, PMA-differentiated *THP-1* M $\Phi$  were washed in ice-cold PBS and lysed using radioimmunoprecipitation assay (RIPA) buffer pH 7.5 (Cell Signaling Technology, Frankfurt, Germany), containing protease/phosphatase inhibitor cocktail (Cell Signaling Technology). The protein concentrations were determined spectrophotometrically using the Pierce BCA (bicinchoninic acid) Protein Assay (Thermo Scientific, Rockford, USA). Proteins were loaded on NuPAGE<sup>®</sup> Novex<sup>®</sup> 4–12% Bis-Tris Gels, pre-cast polyacrylamide gels (Life Technologies GmbH, Darmstadt Germany). Proteins were transferred onto 0.45  $\mu$ m nitrocellulose membranes (Millipore, Billerica, MA, USA). Primary antibodies (Supplemental Table 1) were added and incubated overnight at 4 °C in blocking buffer (5% fat-free milk). Membranes were incubated with enhanced ECL-anti-goat IgG-POD antibody, ECL-anti-mouse IgG-POD antibody or ECL-anti-rabbit IgG-POD antibody. The peroxidase reaction was visualized by AceGlow chemiluminescence substrate (PEQLAB GmbH, Erlangen, Germany) and documented by the Fusion-SL Advance<sup>™</sup> imaging system (PEQLAB GmbH),

according to the manual instructions. The intensity of the specific Western blot bands was quantified using the software ImageJ from the National Institutes of Health (Bethesda, USA) and normalized against  $\alpha$ -tubulin.

## 2.5. Reverse transcription and quantitative polymerase chain reaction

Total RNA was extracted from human *THP-1 MΦ* using PeqGold TRIFast™ (PEQLAB GmbH). DNase I (RNase-free; Thermo Scientific) was used according to the manufacturer's instructions. The AffinityScript Multiple Temperature Reverse Transcriptase and the Brilliant III Ultra-Fast SYBR® Green Master Mix were obtained from Agilent Technologies Deutschland GmbH. (Waldbronn, Germany). All primers were purchased from QIAGEN GmbH (Hilden, Germany) (Supplemental Table 2). RNA concentration and purity were determined by absorbance measurements at 260 nm and 280 nm ( $A_{260}/A_{280} = 1.7\text{--}2.0$ ) using a NanoDrop 8000 Spectrophotometer (Thermo Scientific, Schwerte, Germany). Total RNA integrity was confirmed by lab-on-a-chip technology, using an RNA 6000 NanoChip kit on an Agilent 2100 Bioanalyzer (Agilent Technologies Deutschland GmbH). RNA was only used with an RNA Integrity Number (RIN) of  $8.5 \pm 0.9$ . 1.0  $\mu\text{g}$  of template RNA was used for cDNA synthesis; RNA was reverse transcribed using Oligo(dT)<sub>12-18</sub> primer and the AffinityScript™ Multiple Temperature Reverse Transcriptase, according to the manufacturer's instructions. The cDNA (diluted 1:20) was amplified using the Brilliant III Ultra-Fast SYBR® Green QRT-PCR Master Mix (Stratagene-Agilent Technologies, Waldbronn, Germany). Amplification and data analyses were performed using the Mx3005P™ QPCR System (Stratagene). The data were analyzed using the relative standard curve method. The NormFinder software program was used to ascertain the most suitable reference gene to normalize the RNA input as described earlier [23].

## 2.6. Oil Red O staining

The Oil Red O [ORO, (Sigma-Aldrich Chemie GmbH)] working solution was prepared by diluting the stock solution (3 mg/ml ORO dissolved in 2-propanol) with distilled water (3:2). For staining, PMA differentiated *THP-1 MΦ* were fixed in 10% paraformaldehyde (PFA), and after washing with PBS, the ORO working solution was added to the culture dishes. The nuclei were counterstained using Crystal violet (Carl Roth GmbH, Karlsruhe, Germany).

## 2.7. Cholesterol/cholesteryl ester quantification

For analysis of total cholesterol (TC), free cholesterol (FC) and cholesteryl ester (CE), *THP-1* cells were cultured in 6-well plates, differentiated into *MΦ*, as described above, and incubated with or without 50  $\mu\text{g}/\text{ml}$  oxLDL for 4 h. TC and FC were determined using the TC/FC Quantification Assay (Abcam plc., Cambridge, UK), according to the manufacturer's protocol. The Fluorometric assay was done at Ex/Em = 535/587 nm by a microplate ELISA-reader (Cytation3, BioTek Instruments GmbH, Germany). TC and FC results are presented in  $\mu\text{g}/\text{ml}$ . CE was determined by subtracting the value of FC from TC.

## 2.8. Immunocytofluorescence confocal laser scanning microscopy

Cells were fixed with ice-cold methanol and permeabilized with 0.1% Triton-X 100 in PBS. Thereafter, the detergent was removed by repeated washing in PBS. Primary antibodies (Supplemental Table 1) were applied in PBS overnight (4 °C). After incubation with secondary antibodies (Supplemental Table 1) and subsequent staining with DAPI, we covered the cells with Immu-Mount™ (Thermo Electron Corporation; Pittsburgh; USA). Images were taken by confocal laser-scanning-microscope Eclipse Ti-E, (Nikon GmbH, Düsseldorf, Germany).

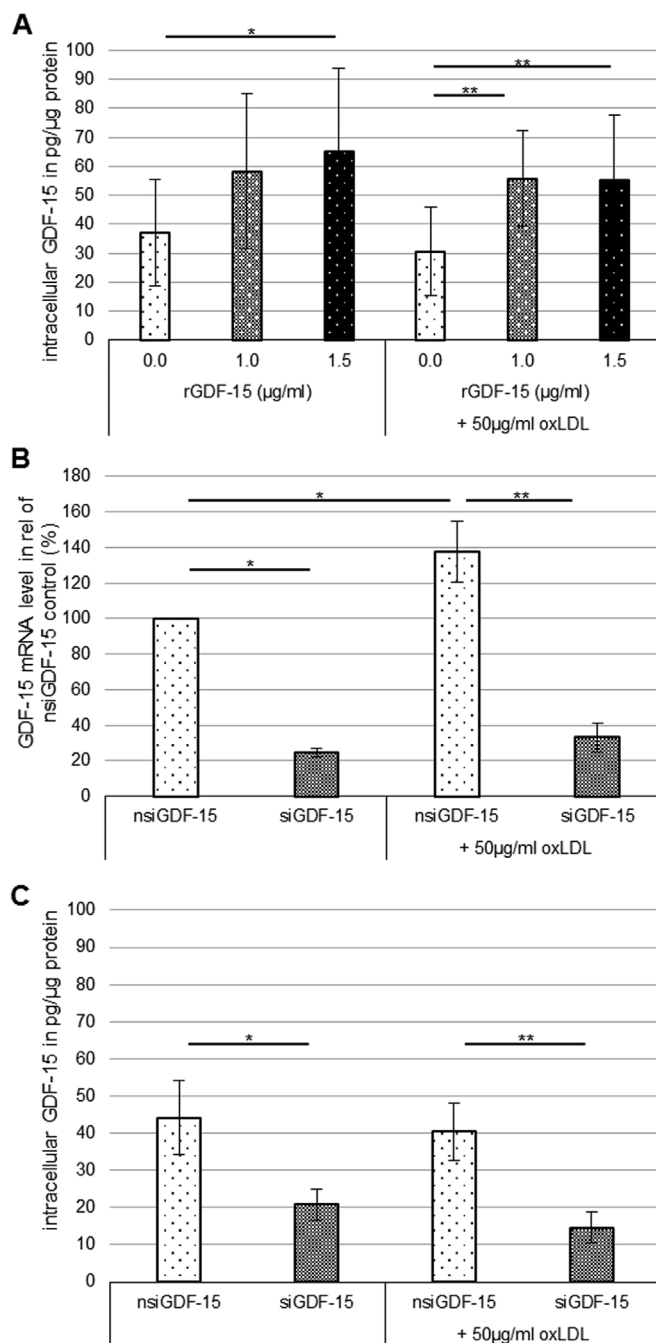


**Fig. 1.** GDF-15 mRNA and protein levels in human *THP-1 MΦ*.

(A) Cellular GDF-15 levels (in pg/μg protein) of *THP-1 MΦ* were determined using ELISA [OD<sub>490/655</sub>] (five independent experiments were performed). (B) Percentage of *GDF-15* mRNA expression levels determined using RT-qPCR in *siGDF-15* or *nsiGDF-15 THP-1 MΦ* (three independent experiments were performed). (C) Cellular GDF-15 levels (in pg/μg protein) of *siGDF-15* or *nsiGDF-15 THP-1 MΦ* were determined using ELISA [OD<sub>490/655</sub>] (six independent experiments were performed). Data are presented as mean ± SD. \* $p \leq 0.05$  significance vs. medium control, \*\* $p < 0.001$  significance vs. oxLDL-treated *MΦ*.

## 2.9. Statistical analyses

Statistical analyses were performed using SigmaPlot 12 (Systat Software Inc., USA). After testing for normality (by Shapiro-Wilk), the unpaired Student's t-test or one-way analysis of variance (ANOVA) was used. Data are reported as mean ± standard error of the mean (SD).  $p < 0.05$  was considered as statistically significant.

### 3. Results

#### 3.1. Impairment of oxLDL on GDF-15 expression in human THP-1 MΦ

To investigate the effects of GDF-15 on the autophagic processes and lipid accumulation, we added recombinant (r)GDF-15 or transiently silenced *GDF-15* in PMA-differentiated human *THP-1 MΦ* (*siGDF-15-MΦ*) (Fig. 1). As negative control, we used a non-silencing siRNA (*nsiGDF-15*) without homology with any known mammalian gene. rGDF-15 resulted in an increase of cellular GDF-15 from  $36.9 \pm 18.5$  pg/μg protein to  $58.2 \pm 26.9$  pg/μg protein ( $p = 0.09$  vs. medium control) using 1.0 μg/ml rGDF-15 or  $65.3 \pm 28.6$  pg/μg protein ( $p = 0.03$  vs. medium control) using 1.5 μg/ml rGDF-15 (Fig. 1A). The transient transfection achieved a significant ( $p < 0.03$  vs. *nsiGDF-15*) knock-down of *GDF-15*, i.e. *GDF-15* mRNA levels decreased from 100% to  $25\% \pm 2.5\%$  ( $-75\%$ ;  $p = 0.029$ ) (Fig. 1B) and protein levels decreased from  $44.2 \pm 10.1$  pg/μg protein to  $20.9 \pm 4.2$  pg/μg protein ( $-53\%$ ;  $p = 0.026$ ) compared with control (*nsiGDF-15*) (Fig. 1C). Additionally, exposure of *nsiGDF-15 MΦ* to 50 μg/ml oxLDL for 4 h resulted in a  $37.0\% \pm 17.2\%$  ( $p < 0.001$ ) higher *GDF-15* mRNA expression in comparison with medium control (Fig. 1B), whereas this significant oxLDL-induced increase in *GDF-15* mRNA levels was not seen in *siGDF-15 MΦ* in comparison with *siGDF-15 MΦ* cultured in medium alone (Fig. 1B). However, the exposure (4 h) of *THP-1 MΦ*, *siGDF-15*- or *nsiGDF-15 MΦ* to 50 μg/ml oxLDL had no effect on GDF-15 protein levels (Fig. 1A and C).

#### 3.2. GDF-15 impairs the cellular lipid content in human THP-1 MΦ

Mice MΦ are able to process intracellular lipids via the autophagy-lysosome pathway [24]. For this reason, we analyzed by ORO-staining whether the intracellular lipid-storage is dependent on GDF-15 in human *THP-1 MΦ*. After addition of rGDF-15, the cellular lipid content in *THP-1 MΦ* significantly ( $p < 0.05$ ) increased (1.0 μg/ml rGDF-15:  $109\% \pm 14.8\%$ ; 1.5 μg/ml rGDF-15:  $117\% \pm 11.9\%$ ) compared to *THP-1 MΦ* cultured in medium alone (Fig. 2A and C–D). *Vice versa*, in *siGDF-15 MΦ* cultured in medium, we found a significant ( $p = 0.02$ )  $-19\% \pm 13.9\%$  decrease of the cellular lipid content (Fig. 2B, G and H). Moreover, 50 μg/ml oxLDL (4 h) treatment resulted in a significant ( $p < 0.01$ )  $137\% \pm 15.9\%$  increase in lipid accumulation (Fig. 2A, C and E). Additionally, oxLDL treatment led to a significant ( $p \leq 0.028$ ) advanced accumulation of lipids in *nsiGDF-15 THP-1 MΦ* ( $129\% \pm 28.6\%$ ) (Fig. 2B, G and I) and *siGDF-15 THP-1 MΦ* ( $111\% \pm 25.0\%$ ) (Fig. 2B, H and J), whereas oxLDL-treated *siGDF-15 MΦ* showed a significant  $-18\%$  ( $p < 0.05$ ) lower lipid accumulation compared to oxLDL-treated *nsiGDF-15 MΦ* (Fig. 2B and I–J). Certainly, *THP-1 MΦ* co-incubated with rGDF-15/oxLDL did not change the lipid content significantly compared to oxLDL-treated MΦ (Fig. 2A and E–F). Surprisingly, the content total cholesterol (TC), free cholesterol (FC) and cholesterol ester (CE) was unchanged after 4 h oxLDL-stimulation. Furthermore, rGDF-15 and GDF-15-silencing had no effect on TC, FC and CE content in human *THP-1 MΦ* (Fig. 2K–P).

#### 3.3. GDF-15 affects ATG5 protein level and p62 accumulation in human THP-1 MΦ

Autophagic MΦ are found at sites of atherosclerotic lesions, in which the autophagy flux is impaired with lesion progression, indicating a crucial role for autophagy in atherosclerosis [14,15]. Regarding the link between lipid accumulation and autophagy, we further investigated a potential role of GDF-15 on autophagy. Therefore, we examined the expression of autophagy-relevant proteins/complexes ATG5, ATG12/ATG5 and p62 in *THP-1 MΦ* dependent on GDF-15 and oxLDL.

Treatment of *THP-1 MΦ* with oxLDL or rGDF-15 alone for 4 h did not affect the ATG5 and ATG12/ATG5-complex protein (Fig. 3A and B).

Co-incubation of *THP-1 MΦ* with oxLDL/rGDF-15 (4 h) showed a significant ( $p \leq 0.04$ ) increase (1.0 μg/ml rGDF-15: 49%; 1.5 μg/ml rGDF-15: 47%) of ATG5 protein levels (Fig. 3A) compared to rGDF-15-treatment alone. In context, ATG12/ATG5 protein complex increased (1.0 μg/ml rGDF-15: 107%; 1.5 μg/ml rGDF-15: 141%;  $p \leq 0.03$ ) significantly by co-incubation of *THP-1 MΦ* with oxLDL/rGDF-15 (4 h) compared to rGDF-15-treated MΦ (Fig. 3B).

Down-regulation of cellular *GDF-15* in human *THP-1 MΦ* (*siGDF-15 MΦ*) resulted in a significant oxLDL-independent reduction of ATG5 protein (medium-treated *siGDF-15 MΦ* by  $-35\%$  [ $p < 0.05$ ]; oxLDL-treated *siGDF-15 MΦ* by  $-33\%$  [ $p = 0.03$ ]) compared to *nsiGDF-15 MΦ* ( $100\% \pm 15.2\%$ ) (Fig. 3C). ATG12/ATG5-complex was reduced by  $-15\%$  ( $p = 0.03$ ) in *siGDF-15 MΦ* compared to *nsiGDF-15 MΦ* ( $100\% \pm 5.2\%$ ) (Fig. 3D).

As a marker of autophagic status, p62-protein increased in oxLDL-treated *THP-1 MΦ* (*THP-1 MΦ*:  $131\% \pm 36.3\%$  [ $p = 0.065$ ]; *nsiGDF-15 THP-1 MΦ*:  $161\% \pm 70.0\%$  [ $p = 0.03$ ]) (Fig. 4A and B). 1.5 μg/ml rGDF-15 co-incubated with oxLDL further amplified the significant increase of p62-protein of about 66% ( $p < 0.05$ ) compared to oxLDL treatment (Fig. 4A). In this context, without oxLDL, *siGDF-15 THP-1 MΦ* showed a significant ( $p < 0.05$ )  $-33\%$  reduced p62-protein level compared to *nsiGDF-15 THP-1 MΦ* (Fig. 4B).

In addition to our Western blot data, we immunocytochemically investigated the intracellular p62 localization in *THP-1 MΦ* using confocal laser scanning microscopy. We noted that endogenously expressed p62 was present in numerous round bodies (mean size:  $\geq 1.7$  μm) in the perinuclear area, with a diffuse distribution in the cytoplasm of human *THP-1 MΦ* (Fig. 4C–L). For the assessment of the autophagy flux, we analyzed p62 accumulation in *THP-1 MΦ* with or without (~ control) exposure to oxLDL. Starvation analyses of *THP-1 MΦ*, as positive control for a suppressed autophagy flux, showed an increased p62 accumulation (Fig. 4H). 1.5 μg/ml rGDF-15 alone increased ( $126\% \pm 54.7\%$ ;  $p < 0.05$ ) significantly the p62 accumulation in *THP-1 MΦ* compared to medium control (Fig. 4C–D and M). OxLDL-treated *THP-1 MΦ* showed a significant  $148\% \pm 42.8\%$  increase, whereas 1.5 μg/ml rGDF-15 enhanced p62 accumulation of 32% (Fig. 4E–F and M). In addition, we found that p62 accumulation was significantly ( $p < 0.002$ ) reduced by  $-56\%$  in *siGDF-15 MΦ* (Fig. 4I, J and N). OxLDL treatment increased p62 accumulation in *nsiGDF-15* and *siGDF-15 THP-1 MΦ* (*nsiGDF-15 MΦ*: to  $179\% \pm 24.5\%$ ,  $p = 0.01$ ; *siGDF-15 MΦ*: to  $111\% \pm 10.7\%$ ,  $p = 0.013$ ) (Fig. 4I–L and N). Linked to the previous data, *siGDF-15 MΦ* treated with 50 μg/ml oxLDL showed a significantly ( $p < 0.001$ )  $-64\%$  reduced p62 accumulation compared to *nsiGDF-15 MΦ* (Fig. 4K, L and N).

### 4. Discussion

Autophagy is directly involved in lipid homeostasis [25] and has been spotlighted in possible treatment of diseases associated with dyslipidemia, diabetes or atherosclerosis. GDF-15 levels are independently positively correlated with e.g. diabetes, smoking, renal dysfunction and markers of inflammation [26]. The cytokine GDF-15 has been hypothesized to also play a crucial role in cardiovascular diseases [7–9,27] and in the development of atherosclerosis [10,11,17]. Moreover, clinical investigations indicate GDF-15 as a parameter for risk stratification in myocardial infarction and heart failure [28–30]. Most recently, it has been postulated that the relationship between levels of GDF-15 and inflammatory markers in atherosclerotic lesions may be more significant than in circulation [31]. In relation to this, it has been shown that lifetime lack of GDF-15 considerably inhibits lumen stenosis due to less inflammation in the plaques [10]. On the other side, it has been suggested that atherosclerotic lesions produce GDF-15 in an attempt to limit or repair the lesions and thus, when being overexpressed, GDF-15 has an overall protective effect on the atherosclerotic process [11]. Therefore, our present study, which has focused on the intracellular function of GDF-15, is the first one to assign GDF-15

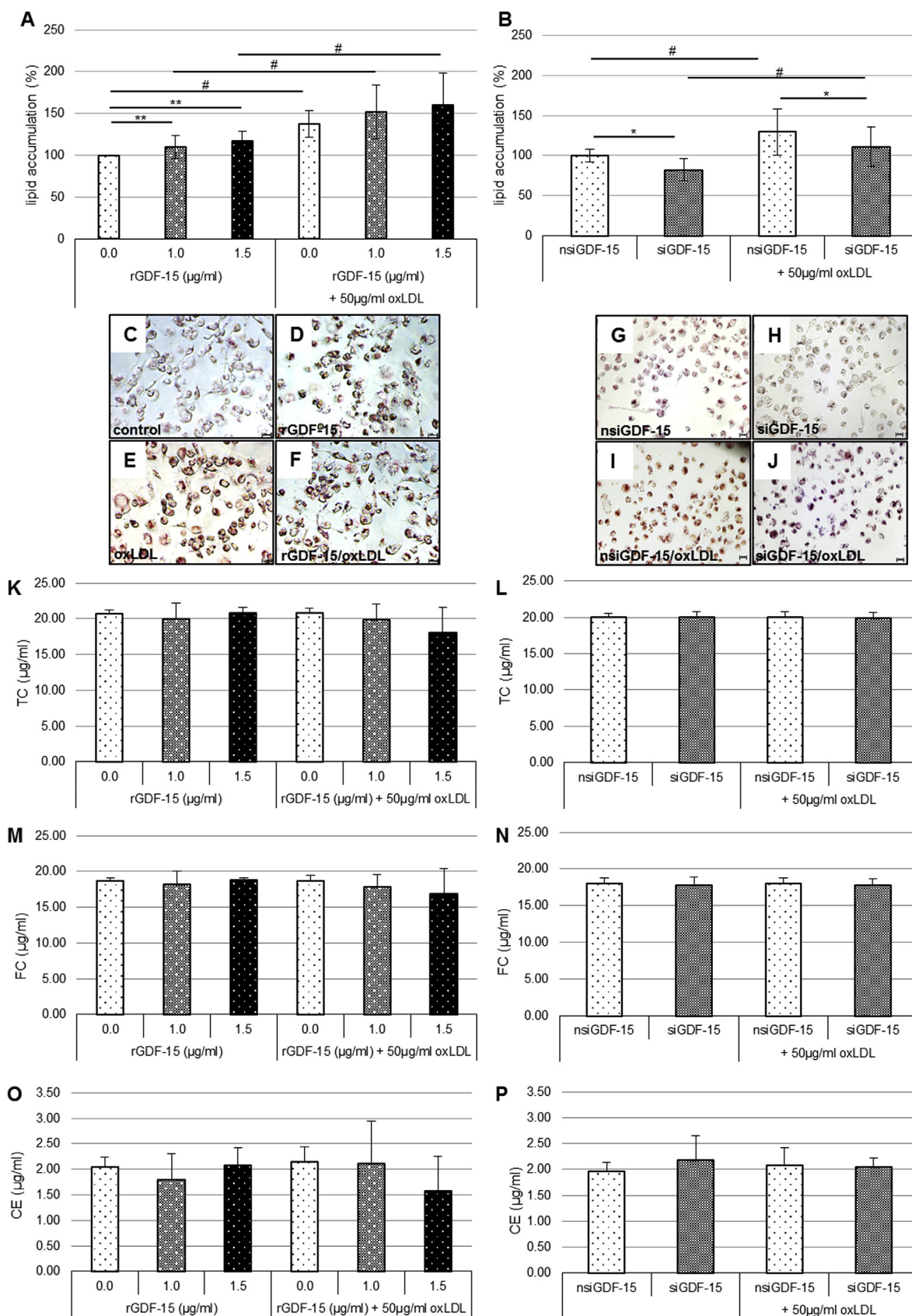


**Fig. 2.** GDF-15 influences the lipid accumulation in *THP-1 MΦ*.

(A and B) Percentage of accumulated lipids quantified and measured by Oil Red O-staining after isopropanol elution [OD<sub>510</sub>] in *THP-1 MΦ*. (C–J) Representative images of Oil Red O-staining in *THP-1 MΦ*. Scale bars: C–F: 100 µm; G–J: 20 µm. Data are presented as mean ± SD (six-seven independent experiments were performed). (K–P) Analyses of (K, L) TC, total cholesterol, (M, N) FC, free cholesterol and (O, P) CE, esterified cholesterol in *THP-1 MΦ*. Results are presented in µg/ml. Data are expressed as mean ± SD of 4 independent experiments. \**p* ≤ 0.05 significance vs. *nsiGDF-15*, #*p* ≤ 0.05 significance vs. without oxLDL; \*\**p* ≤ 0.05 significance vs. medium control.

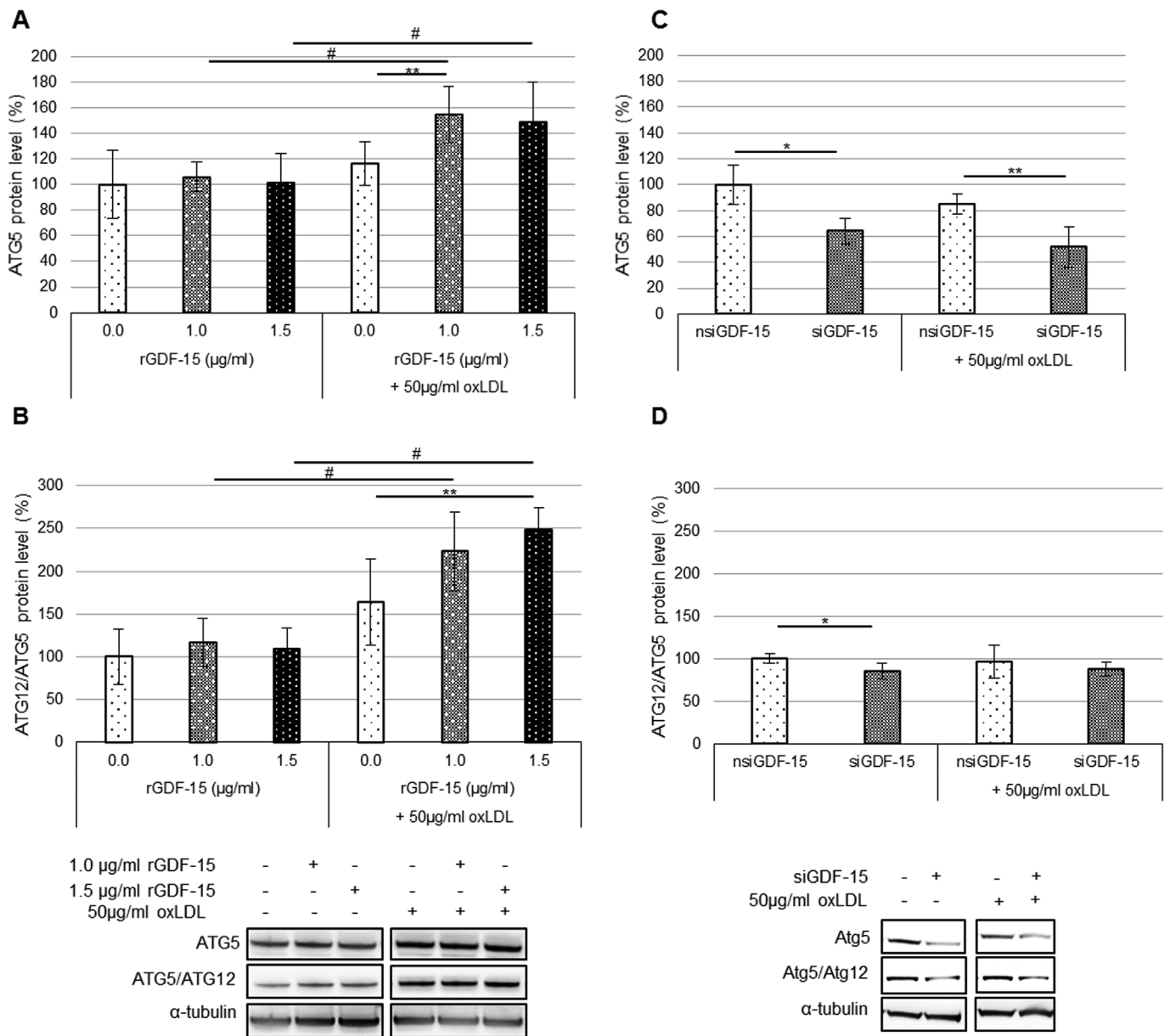
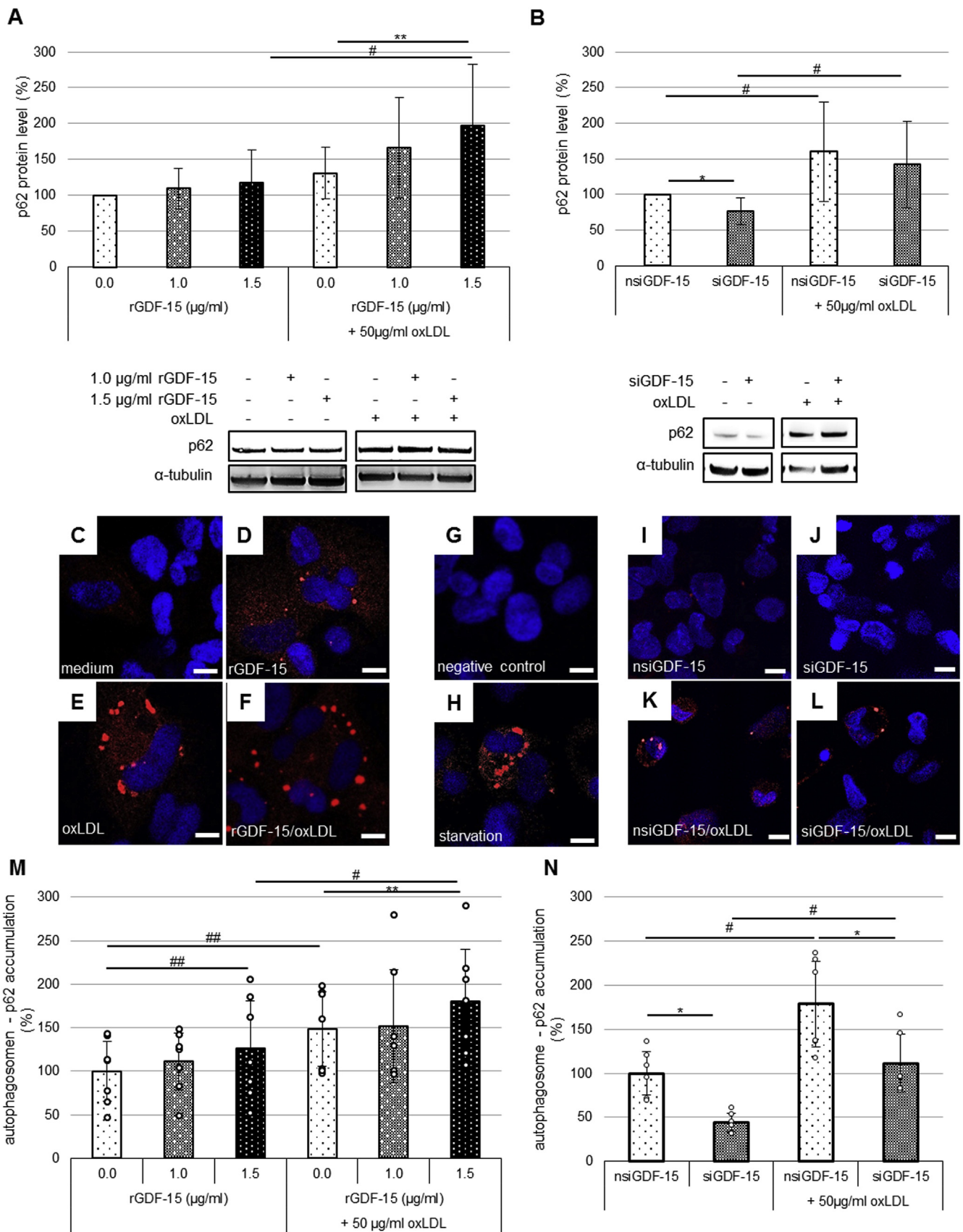


**Fig. 3.** GDF-15 influences the expression of the autophagy-relevant proteins ATG5 and ATG12/ATG5-complex in *THP-1 MΦ*. Percentage of (A and C) Atg5 and (B and D) ATG12/ATG5-complex protein levels in *THP-1 MΦ*. Expression was normalized against  $\alpha$ -tubulin and quantified by ImageJ. Representative images of Western blot results for ATG5, ATG12/ATG5-complex and  $\alpha$ -tubulin. Data are presented as mean  $\pm$  SD (four – six independent experiments were performed). \* $p < 0.05$  significance vs. nsiGDF-15, # $p \leq 0.04$  significance vs. without oxLDL; \*\* $p \leq 0.05$  significance vs. oxLDL-treated *MΦ*. Source data are available online for this figure (see Fig. 1 Ref. [43]).

a pivotal role in autophagy and lipid homeostasis in human *MΦ*, which plays a central role during development and progression of atherosclerotic lesions.

Our study demonstrates that incubation (4 h) of human *THP-1 MΦ* with 50  $\mu$ g/ml oxLDL increased *GDF-15* mRNA expression. These data confirm earlier findings showing or suggesting a link between oxLDL-induced *GDF-15* expression in human *MΦ in vitro* as well as in arteriosclerotic human carotid arteries by co-localization of oxLDL and *GDF-15* immunoreactivity and a significant positive correlation between the percentages of oxLDL and *GDF-15* immunoreactive *MΦ* [7]. However, we show here that rGDF-15 alone increased cellular *GDF-15* protein levels in human *THP-1 MΦ* independent of the addition of oxLDL. Besides this, we observed that rGDF-15 – like oxLDL-increased the intracellular lipid droplets, independent of the addition of oxLDL. In this context, rGDF-15 combined with oxLDL did not aggravate the oxLDL-effect on lipid droplets after 4 h stimulation. Therefore, *THP-1 MΦ* seem

to be saturated using oxLDL, whereby the effect of rGDF-15 (1.5  $\mu$ g/ml) in the presence of oxLDL is not significant. *Vice versa*, silencing of *GDF-15* in human *THP-1 MΦ* (with or without oxLDL) led to reduced cellular lipid accumulation. These data clearly indicate that extra- and intracellular *GDF-15* is directly involved in the regulation of cellular lipid accumulation and, consequently, foam cell formation, whereas the receptor and signaling pathway for *GDF-15* need to be clarified. *MΦ* foam cell formation plays a central pathological role for development/progression of atherosclerotic lesions. Foam cell formation is characterized by an imbalance of cholesterol influx and efflux, accumulation of cholesterol esters (CE) within cytoplasmic lipid droplets and autophagy modulation [32]. In this context, it has been shown that the aggregation of oxLDL inhibits autophagosome elongation and sequestration [15] and induces defective *MΦ* autophagy [12,15]. Interestingly, after a short incubation-time of 4 h, neither oxLDL nor *GDF-15* influenced the TC or CE content of *THP-1 MΦ* in our study. The analysis of lipid



(caption on next page)

**Fig. 4.** GDF-15 influences the expression and accumulation of p62 in *THP-1 MΦ*.

(A and B) Percentage of p62 protein levels in *THP-1 MΦ*. Expression was normalized against  $\alpha$ -tubulin and quantified by ImageJ. Representative images of Western blot results for p62 and  $\alpha$ -tubulin. Data are presented as mean  $\pm$  SD (six - nine independent experiments were performed). (C–L) Representative immunofluorescence images of p62 accumulation (red)/DAPI (blue) double staining in PMA-differentiated human *THP-1 MΦ*, by confocal laser scanning microscopy (Nikon Eclipse). (G) The negative control shows DAPI without secondary antibody against p62. (H) p62 accumulation-positive control was represented by starvation (medium + 2% FKS, 4 h). (M and N) Percentage of p62 accumulation was analyzed with Fiji ImageJ and normalized against DAPI. Each circle represents one independent experiment. Bar graph are presented as mean  $\pm$  SD (six - seven independent experiments were performed). \* $p < 0.05$  significance vs. nsi GDF-15, # $p < 0.05$  significance vs. without oxLDL, \*\* $p < 0.05$  significance vs. oxLDL-treated *MΦ*, ## $p < 0.05$  significance vs. medium control. Source data are available online for this figure (see Fig. 2 Ref. [43]).

droplets using Oil RedO staining detects all neutral lipids, like triacylglycerol (TAG), diacylglycerol (DAG), cholesteryl esters (CE), and free cholesterol (FC). Because of the TC and CE results, we consider that the differences observed using Oil RedO staining might be due to the fraction of TAGs and DAGs. This study shows that rGDF-15 as well as oxLDL increased lipid accumulation in *THP-1 MΦ*. This seems to be an autophagic (lipophagic) process. In addition, oxidative stress via oxLDL increased lipid accumulation by inhibition of the autophagic flux (increased p62 accumulation) [12]. The siGDF-15 analyses suggest that intracellular GDF-15 is important for ATG5 protein expression, with consequences on p62 expression/accumulation and lipid accumulation. In line with this, a recent study has shown that the autophagy activator rapamycin markedly decreased intracellular lipid content during the process of foam cell formation in *THP-1 MΦ* [12]. However, the role of GDF-15 during autophagic or autophagosome formation in *THP-1 MΦ* is not known.

Interestingly, we found that the incubation of human *THP-1 MΦ* with oxLDL plus rGDF-15 results in an increased protein level of ATG5, ATG12/ATG5 and p62, whereas silencing of GDF-15 leads to a reduction of ATG5 and p62 accumulation. However, as a note of caution, it is to refer that there is a discrepancy among our findings showing no significant effects on ATG12/ATG5 ratio in regular *THP-1* macrophages when rGDF-15 is added (without oxLDL), and ATG12/ATG5 ratio increased upon rGDF15 after oxLDL incubation, whereas, unexpectedly, in siGDF-15 macrophages, we found a decrease in ATG12/ATG5 ratio as well as no significant effects on ATG12/ATG5 ratio in oxLDL-treated siGDF-15 macrophages. In general, p62-protein, which regulates cell survival over packing and delivery of polyubiquitinated, misfolded, aggregated proteins and dysfunctional organelles [33–35], is used as marker of the autophagic status [36–39]. It seems that rGDF-15 promotes the autophagosome formation under oxLDL-condition; i.e. increases of ATG5 protein levels or ATG12/ATG5-complex. For these reasons, the increased autophagosome formation triggered by rGDF-15 in oxLDL-treated *THP-1 MΦ* increased p62 accumulation. On the other hand, we showed that *GDF-15* silencing in human *THP-1 MΦ* resulted in decreased protein levels of ATG5, ATG12/ATG5-complex and, as well as p62, including a decreased p62 accumulation, indicating that GDF-15 is involved in the regulation of these autophagy-relevant proteins. In comparison to oxLDL-treated nsiGDF-15 *THP-1 MΦ*, oxLDL-treated siGDF-15 *THP-1 MΦ* showed a reduced p62 accumulation possibly due to the decreased ATG5 levels, because ATG5 and ATG12 promote autophagosome formation and are required for the induction of autophagy [40]. This GDF-15-effect on ATG5 and ATG12/ATG5-complex seems to be a cell survival signaling by oxidative stress, because mice with macrophages-specific deletion of *Atg5*, develop plaques with increased apoptosis and oxidative stress and exhibit enhanced plaque necrosis [16].

The present data show that GDF-15 plays an important role during cytoprotective autophagy. Cytoprotective autophagy would constitute an initial barrier against apoptosis when stress, e.g. oxidative stress, intensity is low [41]. As stress conditions increase, the induction of apoptosis results in the damage of cytoprotective mechanisms by cleavage of essential ATG proteins [41] and consequently an inhibition of the autophagic flux. In addition, autophagy is associated with cell fate in macrophages-derived foam cell formation [12].

Autophagic processes are a novel perspective to understand the

mechanism for plaque progression and stability. Therefore, this study shows that the biomarker GDF-15 is able to regulate autophagy, which may have an important pathophysiological consequence in atherosclerosis. Our study provides an evidence for development of methods for the diagnosis and treatment of atherosclerosis, in agreement with a recent publication [42]. However, because our data were obtained from an atherosclerosis mouse model [10] and *in vitro* investigations using a human monocytic cell line and artificially oxidized LDL, our findings await clinical confirmation.

### Conflicts of interest

The authors declared they do not have anything to disclose regarding conflict of interest with respect to this manuscript.

### Author contributions

Conception and design of the study: AS, KR. Acquisition and analysis of data: KA, AS. Drafting the manuscript: KA, AS. Critical review of manuscript: RK, GB.

### Acknowledgements

We thank Anne Henkeler, Andrea Cordes, Elke Völck-Badouin and Gabriella Stauch for excellent technical assistance.

### Appendix A. Supplementary data

Supplementary data to this article can be found online at <https://doi.org/10.1016/j.atherosclerosis.2018.12.009>.

### References

- [1] A. Schober, M. Böttner, J. Strelau, R. Kinscherf, G.A. Bonaterra, M. Barth, L. Schilling, W.D. Fairlie, S.N. Breit, K. Unsicker, Expression of growth differentiation factor-15/macrophage inhibitor cytokine-1 (GDF-15/MIC-1) in the perinatal, adult, and injured rat brain, *J. Comp. Neurol.* 439 (2001) 32–45.
- [2] M. Bootcov, A. Bauskin, S.M. Valenzuela, A.G. Moore, M. Bansal, X.Y. He, H.P. Zhang, M. Donnellan, S. Mahler, K. Pryor, B.J. Walsh, F.C. Nicholson, W.D. Fairlie, S.B. Por, J.M. Robbins, S.N. Breit, MIC-1, a novel macrophage inhibitory cytokine, is a divergent member of the TGF- $\beta$  superfamily, *Proc. Natl. Acad. Sci.* 94 (1997) 11514–11519.
- [3] W.D. Fairlie, A.G. Moore, A.R. Bauskin, P.K. Russell, H.P. Zhang, S.N. Breit, MIC-1 is a novel TGF- $\beta$  superfamily cytokine associated with macrophage activation, *J. Leukoc. Biol.* 65 (1999) 2–5.
- [4] M. Böttner, M. Laaf, B. Schechinger, G. Rappold, K. Unsicker, C. Suter-Crazzolara, Characterization of the rat, mouse, and human genes of growth/differentiation factor-15/macrophage inhibiting cytokine-1 (GDF-15/MIC-1), *Gene* 237 (1999) 105–111.
- [5] K. Unsicker, B. Spittau, K. Kriegelstein, The multiple facets of the TGF- $\beta$  family cytokine growth/differentiation factor-15/macrophage inhibitory cytokine-1, *Cytokine Growth Factor Rev.* 24 (4) (2013) 373–384, <https://doi.org/10.1016/j.cytogfr.2013.05.003>.
- [6] W.D. Fairlie, P.K. Russell, A.G. Moore, H.-P. Zhang, P.K. Brown, S.N. Breit, Epitope mapping of the transforming growth factor- $\beta$  superfamily protein, macrophage inhibitory cytokine-1 (MIC-1): identification of at least five distinct epitope specificities, *Biochemistry* 40 (2001) 65–73.
- [7] D. Schlittenhardt, A. Schober, J. Strelau, G.A. Bonaterra, W. Schmiedt, K. Unsicker, J. Metz, R. Kinscherf, Involvement of growth differentiation factor-15/macrophage inhibitory cytokine-1 (GDF-15/MIC-1) in oxLDL-induced apoptosis of human macrophages in vitro and in arteriosclerotic lesions, *Cell Tissue Res.* 318 (2004) 325–333, <https://doi.org/10.1007/s00441-004-0986-3>.

- [8] D.A. Brown, S.N. Breit, J. Buring, W.D. Fairlie, A.R. Bauskin, T. Liu, P.M. Ridker, Concentration in plasma of macrophage inhibitory cytokine-1 and risk of cardiovascular events in women: a nested case-control study, *Lancet* 359 (2002) 2159–2163.
- [9] J.F. Lin, S. Wu, S.Y. Hsu, K.H. Yeh, H.H. Chou, S.T. Cheng, T.Y. Wu, W.T. Hsu, C.C. Yang, Y.L. Ko, Growth-differentiation factor-15 and major cardiac events, *Am. J. Med. Sci.* 347 (4) (2014) 305–311.
- [10] G.A. Bonaterra, S. Zügel, J. Thøgersen, S.A. Walter, U. Haberkorn, J. Strelau, R. Kinscherf, Growth differentiation factor-15 deficiency inhibits atherosclerosis progression by regulating interleukin-6-dependent inflammatory response to vascular injury, *J. Am. Heart Assoc.* 1–14 (2012), <https://doi.org/10.1161/JAHA.112.002550>.
- [11] H. Johnen, T. Kuffner, D.A. Brown, B.J. Wub, R. Stocker, S.N. Breit, Increased expression of the TGF- $\beta$  superfamily cytokine MIC-1/GDF15 protects ApoE(-/-) mice from the development of atherosclerosis, *J. Car Path* 21 (2012) 499–505, <https://doi.org/10.1016/j.carpath.2012.02.003>.
- [12] X. Liu, Y. Tang, Y. Cui, H. Zhang, D. Zhang, Autophagy is associated with cell fate in the process of macrophage-derived foam cells formation and progress, *J. Biomed. Sci.* 23 (2016) 57, <https://doi.org/10.1186/s12929-016-0274-z>.
- [13] N. Mizushima, M. Komatsu, Autophagy: renovation of cells and tissue, *Cell* 147 (4) (2011) 728–741.
- [14] B. Razani, C. Feng, T. Coleman, R. Emanuel, H. Wen, S. Hwang, J.P. Ting, H.W. Virgin, M.B. Kastan, C.F. Semenkovich, Autophagy links inflammasomes to atherosclerotic progression, *Cell Metabol.* 15 (4) (2012) 534–544.
- [15] F. Zhou, D. Liu, H.F. Ning, X.C. Yu, X.R. Guan, The roles of p62/SQSTM1 on regulation of matrix metalloproteinase-9 gene expression in response to oxLDL in atherosclerosis, *Biochem. Biophys. Res. Commun.* 472 (2016) 451–458, <https://doi.org/10.1016/j.bbrc.2016.01.065>.
- [16] X. Liao, J.C. Sluimer, Y. Wang, M. Subramanian, K. Brown, J.S. Pattison, J. Robbins, J. Martinez, I. Tabas, Macrophage autophagy plays a protective role in advanced atherosclerosis, *Cell Metabol.* 15 (4) (2012) 545–553.
- [17] M.R. Preusch, M. Baeuerle, C. Albrecht, E. Blessing, M. Bischof, H.A. Katus, F. Bea, GDF-15 protects from macrophage accumulation in a mouse model of advanced atherosclerosis, *Eur. J. Med. Res.* 18 (2013) 19 <http://www.eurjmedres.com/content/18/1/19>.
- [18] J. Galle, C. Wanner, Oxidized LDL and Lp(a). Preparation, modification, and analysis, *Methods Mol. Biol.* 108 (1998) 119–130, <https://doi.org/10.1385/0-89603-472-0:119>.
- [19] U.P. Steinbrecher, Oxidation of human low density lipoprotein results in derivatization of lysine residues of apolipoprotein B by lipid peroxide decomposition products, *J. Biol. Chem.* 262 (8) (1987) 3603–3608.
- [20] K.K. Foxx, R.L. Roberts, M.J. Waxdal, Effect of Copper Ion Concentration on the Oxidation of Human LDL, Kalen Biomedical, LLC, 2008.
- [21] M. Loughheed, U.P. Steinbrecher, Mechanism of uptake of copper-oxidized low density lipoprotein in macrophages is dependent on its extent of oxidation, *J. Biol. Chem.* 271 (20) (1996) 11798–11805.
- [22] S. Tsuchiya, M. Yamabe, Y. Yamaguchi, Y. Kobayashi, T. Konno, K. Tada, Establishment and characterization of a human acute monocytic leukemia cell line (THP-1), *Int. J. Canc.* 26 (2) (1980) 171–176.
- [23] J. Stern-Straeter, G.A. Bonaterra, K. Hormann, R. Kinscherf, U.R. Goessler, Identification of valid reference genes during the differentiation of human myoblasts, *BMC* 10 (2009) 66, <https://doi.org/10.1186/1471-2199-10-66>.
- [24] M. Ouimet, V. Franklin, E. Mak, X. Liao, I. Tabas, Y.L. Marcel, Autophagy regulates cholesterol efflux from macrophage foam cells via lysosomal acid lipase, *Cell Metabol.* 13 (6) (2011) 655–667, <https://doi.org/10.1016/j.cmet.2011.03.023>.
- [25] R. Singh, S. Kaushik, Y. Wang, Y. Xiang, I. Novak, M. Komatsu, K. Tanaka, A.M. Cuervo, M.J. Czaja, Autophagy regulates lipid metabolism, *Nature* 458 (7242) (2009) 1131–1135, <https://doi.org/10.1038/nature07976>.
- [26] J.M. Kim, M.K. Back, H.S. Yi, K.H. Joung, H.J. Kim, B.J. Ku, Effect of atorvastatin on growth differentiation factor-15 in patients with type 2 diabetes mellitus and dyslipidemia, *Diabetes Metab. J* 40 (1) (2016) 70–78, <https://doi.org/10.4093/dmj.2016.40.1.70>.
- [27] S. Zügel, S. Vorwald, G. Bendner, G.A. Bonaterra, J. Strelau, R. Kinscherf, Effect of gdf-15 (growth differentiation factor 15) in the progression of atherosclerosis, *Atherosclerosis Suppl.* 11 (2) (2010) 1–15.
- [28] T. Kempf, M. Eden, J. Strelau, M. Naguib, C. Willenbockel, J. Tongers, J. Heineke, D. Kotlarz, J. Xu, J.D. Molkenin, H.W. Niessen, H. Drexler, K.C. Wollert, The transforming growth factor-15 superfamily member growth-differentiation factor-15 protects the heart from ischemia/reperfusion injury, *Circ. Res.* 98 (2006) 351–360.
- [29] T. Kempf, E. Björklund, S. Olofsson, B. Lindahl, T. Allhoff, T. Peter, J. Tongers, K.C. Wollert, L. Wallentin, Growth-differentiation factor-15 improves risk stratification in ST-segment elevation myocardial infarction, *Eur. Heart J.* 28 (2007) 2858–2865, <https://doi.org/10.1093/eurheartj/ehm465>.
- [30] K.C. Wollert, T. Kempf, B. Lagerqvist, B. Lindahl, S. Olofsson, T. Allhoff, T. Peter, A. Siegbahn, P. Venge, H. Drexler, L. Wallentin, Growth differentiation factor 15 for risk stratification and selection of an invasive treatment strategy in non-ST-elevation acute coronary syndrome, *Circulation* 116 (2007) 1540–1548.
- [31] J. Chen, F. Luo, Z. Fang, W. Zhang, GDF-15 levels and atherosclerosis, *Int. J. Cardiol.* 15 (257) (2018) 36, <https://doi.org/10.1016/j.ijcard.2017.10.037>.
- [32] J. He, G. Zhang, Q. Pang, C. Yu, J. Xiong, J. Zhu, F. Chen, SIRT6 reduces macrophage foam cell formation by inducing autophagy and cholesterol efflux under oxLDL condition, *FEBS J.* 284 (9) (2017) 1324–1337, <https://doi.org/10.1111/febs.14055> Epub 2017 Mar 31.
- [33] S. Pankiv, T.H. Clausen, T. Lamark, A. Brech, J.A. Bruun, H. Outzen, A. Overvatn, G. Bjorkoy, T. Johansen, p62/SQSTM1 binds directly to atg8/LC3 to facilitate degradation of ubiquitinated protein aggregates by autophagy, *J. Biol. Chem.* 282 (2007) 24131–24145.
- [34] P.K. Kim, D.W. Hailey, R.T. Mullen, J. Lippincott-Schwartz, Ubiquitin signals autophagic degradation of cytosolic proteins and peroxisomes, *Proc. Natl. Acad. Sci. U.S.A.* 105 (2008) 20567–20574.
- [35] V. Kirkin, T. Lamark, Y.S. Sou, G. Bjorkoy, J.L. Nunn, J.A. Bruun, E. Shvets, D.G. McEwan, T.H. Clausen, P. Wild, I. Bilusic, J.P. Theurillat, A. Øvervatn, T. Ishii, J. Elazar, M. Komatsu, I. Dikic, T. Johansen, A role for NBR1 in autophagosomal degradation of ubiquitinated substrates, *Mol. Cell* 33 (2009) 505–516.
- [36] G. Bjorkoy, T. Lamark, A. Brech, H. Outzen, M. Perander, A. Øvervatn, H. Stenmark, T. Johansen, P62/SQSTM1 forms protein aggregates degraded by autophagy and has a protective effect on huntingtin-induced cell death, *JCB* 171 (4) (2005) 603–614, <https://doi.org/10.1083/jcb.200507002>.
- [37] M. Komatsu, S. Waguri, M. Koike, Y.S. Sou, T. Ueno, T. Hara, N. Mizushima, J. Iwata, J. Ezaki, S. Murata, J. Hamazaki, Y. Nishito, S. Lemura, T. Natsume, T. Yanagawa, J. Uwayama, E. Warabi, H. Yoshida, T. Ishii, A. Kobayashi, et al., Homeostatic levels of p62 control cytoplasmic inclusion body formation in autophagy-deficient mice, *Cell* 131 (2007) 1149–1163, <https://doi.org/10.1016/j.cell.2007.10.035>.
- [38] D.J. Klionsky, E.H. Baehrecke, J.H. Brumell, C.T. Chu, P. Codogno, A.M. Cuervo, J. Debnath, V. Deretic, Z. Elazar, E.L. Eskelinen, S. Finkbeiner, J. Fuyo-Margareto, D.A. Gewirtz, M. Jäättelä, G. Kroemer, B. Levine, T.J. Melia, N. Mizushima, D.C. Rubinsztein, A. Simonsen, et al., A comprehensive glossary of autophagy-related molecules and processes, *Autophagy* 7 (11) (2011) 1273–1294, <https://doi.org/10.4161/auto.7.11.17661>.
- [39] R. Mathew, C.M. Karp, B. Beaudoin, N. Vuong, G. Chen, H.Y. Chen, K. Bray, A. Reddy, G. Bhanot, C. Gelinas, R.S. DiPaola, V. Karantza-Wadsworth, E. White, Autophagy suppresses tumorigenesis through elimination of p62, *Cell* 137 (2009) 1062–1075, <https://doi.org/10.1016/j.cell.2009.03.048>.
- [40] J. Romanov, M. Walczak, I. Ibricic, S. Schüchner, E. Ogris, C. Kraft, S. Martens, Mechanism and functions of membrane binding by the Atg5–Atg12/Atg16 complex during autophagosome formation, *EMBO* 31 (2012) 4304–4317, <https://doi.org/10.1038/emboj.2012.278>.
- [41] G. Marino, M. Niso-Santano, E.H. Baehrecke, G. Kroemer, Self-consumption: the interplay of autophagy and apoptosis, *Nat. Rev. Mol. Cell Biol.* 15 (2) (2014) 81–94, <https://doi.org/10.1038/nrm3735>.
- [42] I. Sergin, T.D. Evans, X. Zhang, S. Bhattacharya, C.J. Stokes, E. Song, S. Ali, B. Dehestani, K.B. Holloway, P.S. Micevych, A. Javaheri, J.R. Crowley, A. Ballabio, J.D. Schilling, S. Epelman, C.C. Weihl, A. Diwan, D. Fan, M.A. Zayed, B. Razani, Exploiting macrophage autophagy-lysosomal biogenesis as a therapy for atherosclerosis, *Nat. Commun.* 8 (2017) 15750, <https://doi.org/10.1038/ncomms15750>.
- [43] Ackermann K, Bonaterra GA, Kinscherf R, Schwarz A. Data on Autophagy Marker in Human Macrophages Exposed to OxLDL and Growth Differentiation Factor-15. *Atherosclerosis Data in Brief* (submitted).